Development of a Monostatic, Multifrequency Electromagnetic Mine Detector

Dean A. Keiswetter, Elena Novikova, I.J. Won
Thomas M. Hall, and David Hanson

Geophex, Ltd., 605 Mercury Street, Raleigh, NC 27603

ABSTRACT

A new, monostatic, broadband, electromagnetic sensor, known as the GEM-3M, has been prototyped and tested at various sites containing buried unexploded ordnance (UXO) and mines. The instrument consists of a pair of concentric, circular coils that transmit a continuous, broadband, digitally controlled, electromagnetic waveform. The two transmitter coils, with precisely computed dimensions and placement, create a zone of magnetic cavity (viz., an area with a vanishing primary magnetic flux) at the center of the two coils. A third receiving coil is placed within this magnetic cavity such that it senses only the weak, secondary field returned from the earth and buried target(s). The mine detector is designed for ordinary soldiers and, when completed, will have the following unique features:

- One-man portable high-tech mine detector: intelligent, realtime data interpretation and display on a color LCD screen,
- Targets can be metallic mines (positive conductivity targets), nonmetallic mines (negative conductivity targets), or a disturbed soil condition,
- Detection and characterization based on visual color displays, rather than the tonal changes common to current metal detectors,
- Broadband; selectable frequencies for depth scanning suitable for regional soil conditions and geology, and
- All sensor coils housed in a light, circular disk - very similar in appearance to a conventional metal detector.

Introduction

A recent Army technical report[1] discusses the entire suite of mine detection technologies including the metallic mine detector, ground-probing radar, and various sensors based on thermal, biological, vapor, nuclear (energetic photon, thermal neutron, and X-ray), acoustic, and ultraviolet detection. After 80 pages of extensive technical review and assessment of the detection technologies, the conclusions begin with the following paragraph:

> "The acceptable capability currently available to our soldier is a hand held metallic mine detector. None of the other detection requirements have a satisfactory solution on the horizon. The detection solution is not like finding a needle in a haystack, but it is in many cases like finding a particular needle in a haystack of needles."

This emphatic vote for an ordinary and lowly metal detector, however, should not be regarded as a wholehearted endorsement, but is obviously attributed to the lack of near-term, viable options from other mine detection technologies under development. Some obvious deficiencies of a common metal detector are:

1. The detection is commonly based on the tonal changes, thus, is susceptible to the operator's attention span as well as site conditions that depend on the presence of multiple targets, variation in sizes, and the background geology.

D.K. (correspondence): Email: keiswetter@geophex.com; WWW: http://geophex.com; Telephone: 919-839-8515; Fax 919-839-8528

2. Because most metal detectors work at a single, factory-set frequency, they cannot render a 3-D geometry of the target and its emplacement: they are designed to be an audio *bump* finder. Other than tonal change over a target, there is virtually no quantitative interpretation to the data.
3. The detector is used as a 1-D profiler to sweep a 2-D area, thus, the operator must memorize a *tonal history* over the sweep area in order to reoccupy a potential target location.
4. Depth of penetration is limited for given soil conditions, often to a few inches.

Geophex is developing an advanced, next-generation, high-tech metal detector, known as the GEM-3M, that addresses the deficiencies listed above but keeps the attractive features of a metal detector such as lightweight and operational simplicity. The ultimate objective of development effort is to produce and demonstrate a hand-held sensor capable of detecting and characterizing subsurface targets ranging from small, shallow, plastic land mines to large, buried unexploded ordnance (UXO) in realtime. By measuring the target response at multiple transmitter frequencies, the fully-functional GEM-3M detector will be able to characterize a buried mine, metallic or non-metallic, using realtime data-processing software, and display a 3-D target image on a small color LCD screen. This paper describes the GEM-3M design principles and presents field data acquired with a prototype GEM-3M sensor.

GEM-3M Overview

The GEM-3M is designed to use a pair of concentric, circular coils to transmit a continuous, wideband, digital, electromagnetic (EM) waveform. The resulting field induces a secondary current in the earth as well as in any buried mines. The set of two transmitter coils, with precisely computed dimensions and placement, creates a zone of magnetic cavity (i.e., an area with a vanishing primary magnetic flux) at the center of the two coils (Figure 1). A third receiving coil is placed within this magnetic cavity so that it senses only the weak, secondary field returned from the earth and buried targets. All coils are molded into a single, light, circular disk in a fixed geometry, rendering a very portable, monostatic sensor head. The removable electronics package controls system operations and stores the digital data.

The monostatic configuration has many advantages including a compact sensor head, large transmitter moment, high spatial resolution, no spatial distortion of an anomaly common to bistatic sensors, and circular symmetry that greatly simplifies the mathematical description and forward- and inverse-modeling processes. Three prototype GEM-3M units have been built and tested at various environmental sites, including those containing unexploded ordnance and land mines.

The digital design of the GEM-3M allows it to operate at multiple frequencies simultaneously. The importance of multiple frequencies is related to the depth of exploration (also known as the skin depth). The depth of exploration is inversely proportional to frequency: a low-frequency signal travels far through a conductive earth and, thus, senses deep targets, while a high-frequency signal travels only a short distance and, thus, senses only shallow targets[2]. Sweeping through a broadband, therefore, is equivalent to depth scanning and provides the basic EM data for 3-D imaging[3].

The GEM-3M stores the inphase and quadrature response[4,5] in part-per million (ppm). We note that the raw data in ppm is sensor-specific and has little physical meaning. In most shallow geophysical surveys, however, the ppm data generated by GEM-3M are often sufficient to locate buried objects without elaborate data processing or interpretation[3].

The raw data logged by the GEM-3M (viz., inphase and quadrature response in ppm) can be used for inverse processing and imaging[5,6]. (Witten et al., 1997a,b). Traditionally, however, EMI data is displayed in "apparent conductivity" by assuming that the earth below the sensor is represented by a homogeneous and isotropic halfspace. While the earth is heterogeneous with regard to geologic variations, it can be represented by an equivalent homogeneous halfspace that would result in the same observed data[7].

Design of a Magnetic Cavity Using Two Concentric Coils

This section describes the GEM-3M design principle involving two concentric transmitter coils[8]. A magnetic cavity is defined as a region where a directional sensor, placed in a specified orientation, produces zero signal induced from the magnetic field. We show that such a cavity can be created at the center of two concentric, circular, current loops that are electrically connected in series into one circuit. The cavity, once created, can be used for placing a highly sensitive magnetic sensor in the neighborhood of a large active, dipolar magnetic field. The concept is schematically shown in Figure 1.

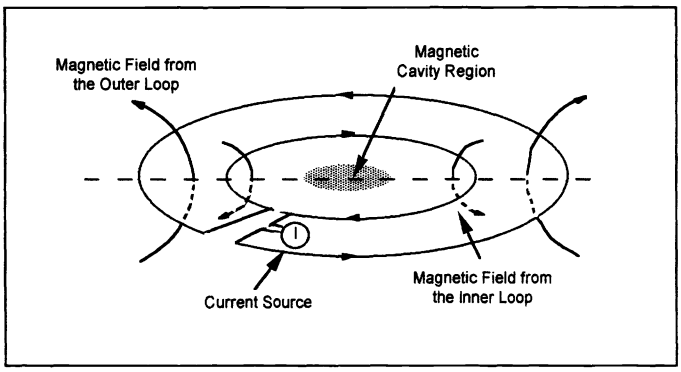

Figure 1. Conceptual representation of creating a central magnetic cavity region using two concentric, circular loops that are electrically connected in an opposing polarity.

Magnetic Field of a Single Circular Loop

Because the magnetic cavity is to be created at the center of a current-carrying loop, we must first analyze the near-field characteristics of the magnetic field generated by a single loop. Let us consider the magnetic field at an arbitrary point $Q(r,\theta)$ off the axis of a circular loop as shown in Figure 2. The loop has a radius a and carries a current I. Owing to the obvious azimuthal symmetry, we can express the scalar magnetic potential function[9] V_m as

$$V_m(r,\theta) = \sum_{n=0}^{\infty} A_n r^n P_n(\cos\theta) + \sum_{n=0}^{\infty} B_n r^{-(n+1)} P_n(\cos\theta) \tag{1}$$

where V_m satisfies Laplace equation $\nabla^2 V_m = 0$ and P_n is the n-th order Legendre function.

For $\theta = 0$, V_m can be analytically shown to be

$$V_m(r = z;\ \theta = 0) = \frac{\mu_0 I}{2}\left(1 - \frac{z}{\sqrt{a^2 + z^2}}\right), \tag{2}$$

which is true for any value z along the axis. Magnetic permeability of free space (μ_0) has a value of $4\pi\cdot 10^{-7}$ henry/m. Eq. (2) may be expanded into a Taylor series in terms of either (a/z) for a<z or (z/a) for a>z. By comparing the coefficients of the power series with those of Eq. (1), we can derive the following two equations:

$$V_m(r,\theta) = \frac{\mu_0 I}{2}\left\{1 - \left(\frac{r}{a}\right)P_1(\cos\theta) + \sum_{n=1}^{\infty}(-1)^{n+1}\frac{(2n-1)!!}{(2n)!!}\left(\frac{r}{a}\right)^{2n+1}P_{2n+1}(\cos\theta)\right\} \quad \text{for } r \le a \tag{3a}$$

and

$$V_m(r,\theta) = \frac{\mu_0 I}{2}\left\{\sum_{n=1}^{\infty}(-1)^{n+1}\frac{(2n-1)!!}{(2n)!!}\left(\frac{a}{r}\right)^{2n}P_{2n-1}(\cos\theta)\right\} \quad \text{for } r \ge a. \tag{3b}$$

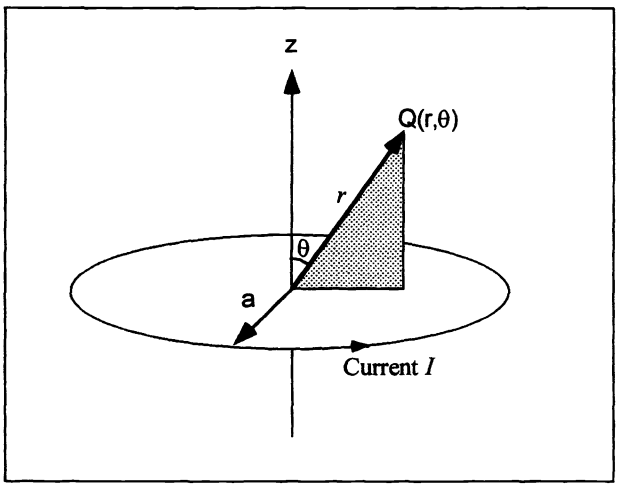

Figure 2. Geometry for computing magnetic field for a single current-carrying circular loop.

Vector magnetic field $\boldsymbol{B}(r,\theta)$ can be derived from the scalar potential function;

$$\boldsymbol{B}(r,\theta) = -\nabla V_m(r,\theta) \tag{4}$$

and B_z, the field perpendicular to the plane of the loop, may be computed by;

$$B_z = -\cos\theta \frac{\partial V_m}{\partial r} + \frac{\sin\theta}{r} \frac{\partial V_m}{\partial \theta}. \tag{5}$$

The partial derivatives of the magnetic potential are:

$$\frac{\partial V_m}{\partial r} = \frac{\mu_0 I}{2a}\left\{ -P_1(\cos\theta) + \sum_{n=1}^{\infty} (-1)^{n+1} \frac{(2n-1)!!}{(2n)!!}(2n+1)\left(\frac{r}{a}\right)^{2n} P_{2n+1}(\cos\theta) \right\}, \text{ for } r \le a; \tag{6a}$$

$$\frac{\partial V_m}{\partial r} = \frac{\mu_0 I}{2a}\left\{ \sum_{n=1}^{\infty} (-1)^{n} \frac{(2n-1)!!}{(2n)!!}(2n)\left(\frac{a}{r}\right)^{2n+1} P_{2n-1}(\cos\theta) \right\}, \text{ for } r \ge a; \tag{6b}$$

and

$$\frac{\partial V_m}{\partial \theta} = \frac{\mu_0 I}{2}\left\{ \left(\frac{r}{a}\right)(\sin\theta) + \sum_{n=1}^{\infty} (-1)^{n} (\sin\theta) \frac{(2n-1)!!}{(2n)!!}\left(\frac{r}{a}\right)^{2n+1} P'_{2n+1}(\cos\theta) \right\}, \text{ for } r \le a; \tag{6c}$$

$$\frac{\partial V_m}{\partial \theta} = \frac{\mu_0 I}{2}\left\{ \sum_{n=1}^{\infty} (-1)^{n} \frac{(2n-1)!!}{(2n)!!}\left(\frac{a}{r}\right)^{2n} (\sin\theta)\, P'_{2n-1}(\cos\theta) \right\}, \text{ for } r \ge a. \tag{6d}$$

The derivative of the Legendre polynomials, $P(\zeta)$, in Eq. (6c) and (6d) are taken with respect to the argument $\zeta = \cos\theta$.

As r approaches zero, B_z approaches $\frac{\mu_0 I}{2a}$, as may be seen from Eq. (5) and Eqs. (6a and 6c). For $r>>a$, the far field approximation is

$$B_z(r) = -\frac{\mu_0 I a^2}{4r^3} = -\frac{\mu_0 M}{4\pi r^3} \quad \text{where } M \text{ (magnetic moment)} = I\pi a^2 \tag{7}$$

in the plane of the loop, and

$$B_z(r) = \frac{\mu_0 I a^2}{2r^3} \tag{8}$$

on the coil axis, which are the classical expressions for a dipolar magnetic field.

The magnetic field at the center of the loop is stable and has a vanishing gradient. This spatial stability is the major asset that enables us to create a magnetic cavity by means of superimposing an opposite, yet also stable, magnetic field generated by a smaller concentric loop.

Creation of a Central Magnetic Cavity Using Two Opposing Current Loops

Figure 1 shows the basic concept of creating a magnetic cavity using two loops of radius a_1 and a_2; a series circuit of two connected loops carrying the same current in opposing directions. The field generated by circulating a current (I) through each transmitter loop is described by Eqs. 5 and 6. If we place a third coil, with radius a_3, inside the inner transmit loop, the voltage output (emf) of this coil is proportional to the surface integral of the two opposing magnetic fields at $\theta = 90$:

$$emf = \int_0^{a_3} [B_z^2(r) - B_z^1(r)] \cdot 2\pi r \, dr. \tag{9}$$

To create the desired magnetic cavity, therefore, the emf must vanish according to:

$$\int_0^{a_3} B_z^1(r)\, r\, dr = \int_0^{a_3} B_z^2(r)\, r\, dr. \tag{10}$$

The mathematical relationship between the radii of the receiver coil and two concentric transmitter coils, as well as the number of turns, that results in zero sensor output voltage in free space is straightforward[5].

Figure 3 shows a simulated magnetic cavity for the case a_1=26 cm, N_1=10, a_2=15.84 cm, and N_2=6, where N is the number of turns. The figure shows the vertical cross-section of the magnetic field strength (normalized to $\frac{\mu_0 I}{2}$). The magnetic cavity, located in the vicinity of r=0 in the plane of the coil system, is easy to identify.

Although the outer coil, which has a larger radius and more turns, is the principal transmitter of an active magnetic field, the inner coil, due to its opposing magnetic polarity, does slightly reduce the amplitude of the principal dipole field. Loss on the dipole strength of the outer coil is proportional to $\frac{a_2^2 N_2}{a_1^2 N_1}$ in the far-field, and is 22% for the example shown in Figure 3.

GEM-3M Field Data Examples

The prototype GEM-3M sensor, shown in Figure 4, resembles a conventional metal detector. Since it debuted in mid-1996, the GEM-3M has been used at many environmental sites. In this section, we present example data that demonstrates the advantages of multifrequency EM data and the importance of inphase and quadrature measurements.

Geophex acquired GEM-3M data at Fort A.P. Hill, VA, in conjunction with a DoD program established to determine the capability of various sensors and processing methods for detecting unexploded ordnance (UXO) and mines. The Night Vision Directorate, U.S. Army, established a test site containing five "registration targets" at precise locations. Each registration area contains an 8-inch aluminum square sheet (north end of registration area) and a 16-lb steel shotput (south

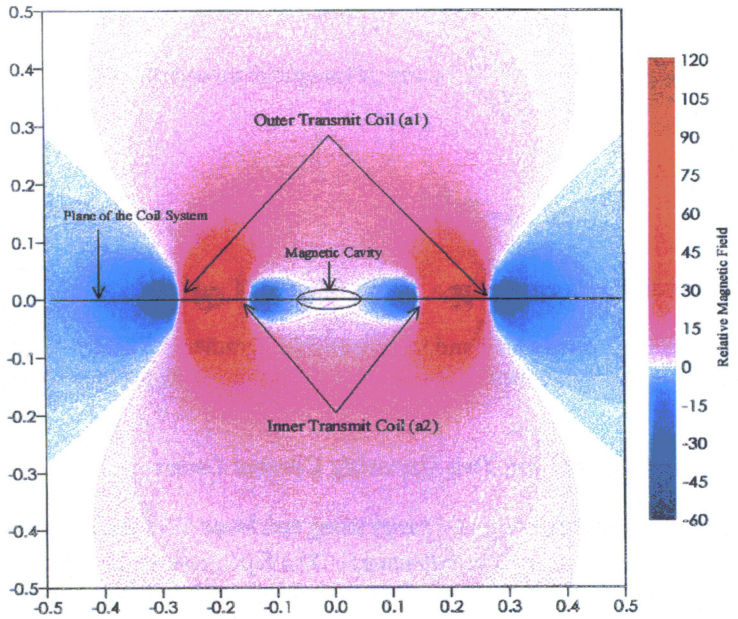

Figure 3. Vertical component of the magnetic field that results from two concentric coils. Notice that the effect of the opposing coil is negligible in the far field. The amplitude scale is normalized to $\frac{\mu_0 I}{2}$.

Figure 4. Photograph of the GEM-3M during a recent field project.

end of registration area). The site, which was known to contain non-emplaced targets, was purposely not cleared prior to the GEM-3M survey in order to determine the effects of environmental clutter on the measured geophysical data.

GEM-3M data were acquired using a vertical magnetic dipole configuration along lines spaced 0.5 meters apart. We used two transmitter frequencies, 4,050 and 12,270 Hz, and recorded the inphase and quadrature response at over 105 thousand locations over the 1.5 acre site. The GEM-3M was configured to acquire data at a 10 Hz sampling rate. The nominal survey method employed a dead-reckoning method, which incorporates continuous recording while walking between two known points at a constant pace. The spatial coordinates of each sampling location are linearly interpolated during post-processing based on the starting and ending locations and the number of data samples acquired along the line. A nominal walking speed resulted in measurements every 20 cm along a survey transect.

The battery-powered GEM-3M sensor stores the data in onboard memory. The data were downloaded to a field computer for data archiving purposes and processing. Commercial software was used to krig and contour the data. Preliminary maps were produced in the field for quality assurance and routine in-field analysis.

The GEM-3M data are shown in Figures 5 and 6. Each of the registration targets (registration areas are identified in Figures 5 and 6 by an open oval) can be identified in these data. In general, the aluminum plate is better observed in the inphase component and the steel shotput is better observed in the quadrature component for both frequencies. Numerous isolated anomalies are observed throughout the site. It is interesting, however, that some of the unidentified anomalies are observed only for a particular frequency and component. We believe that this phenomenon, which we have observed at other sites as well, may prove extremely valuable during discrimination analysis and advanced processing.

Discussion

The GEM-3M sensor is designed to acquire multifrequency EM data and display the results in realtime. This paper only describes the hardware design principles. In addition to hardware issues, we are investigating the (1) optimum method to measure spatial registry data (viz., inertial navigation and global positioning system (DGPS)) and (2) color display technologies. In cooperation with several scientists in the U.S. government and universities, we are also developing robust processing capabilities to enhance realtime interpretations.

A remaining hardware challenge for the continued development of GEM-3M is increasing its operating bandwidth from the present 24 kHz to several hundred kilohertz. Once we can cover a few decades in the frequency band employing an active EMI source, we should be able to measure a continuous spectral response of a given buried object. This can be achieved by either (1) sweeping through the entire bandwidth one frequency at a time[2], or (2) employing a fast Fourier transform technique during the data acquisition using a broadband source such as pseudo-random sequence pulses. Such a concept may be called EMI spectroscopy (EMIS), which may cover ELF to RF spectral bands. Like any other spectroscopic technology, EMIS has an enormous potential for target identification and discrimination, which is the ultimate sensor requirement for many detection applications involving land mines, airport security, and ancillary object identification needs.

Conclusions

GEM-3M is a new, monostatic, broadband, electromagnetic sensor for subsurface geophysical investigation. The sensor is based on a well-founded physical principle of creating a magnetic cavity using two concentric transmitter coils. A receiver coil is placed within this magnetic cavity so that it can sense the weak, secondary field returned from the earth and buried targets. This monostatic configuration has many advantages including compact sensor head, a large transmitter moment, high spatial resolution, no spatial distortion of an anomaly (as is common with bistatic sensors), circular symmetry that greatly simplifies the mathematical description and forward- and inverse-modeling processes.

Three prototype GEM-3M units have been built and tested at various environmental sites, including those containing unexploded ordnance and land mines. The high spatial resolution and quality of these data demonstrates the advantages of the coil design and multifrequency capability.

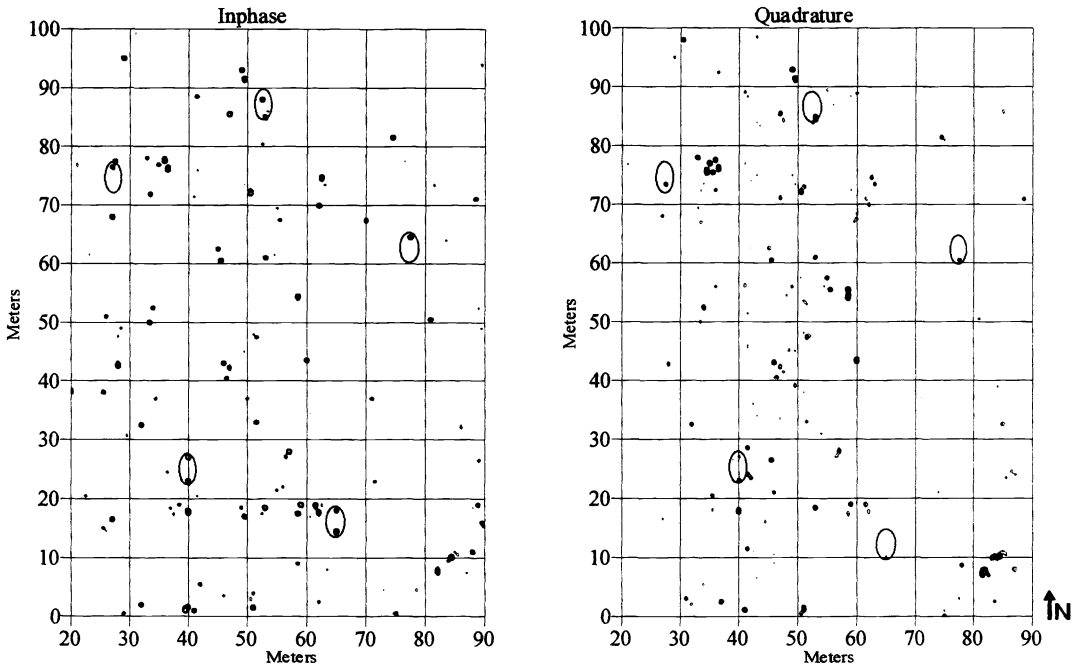

Figure 5. GEM-3M data; 4,050 Hz. The open ovals indicate the locations of the registration targets.

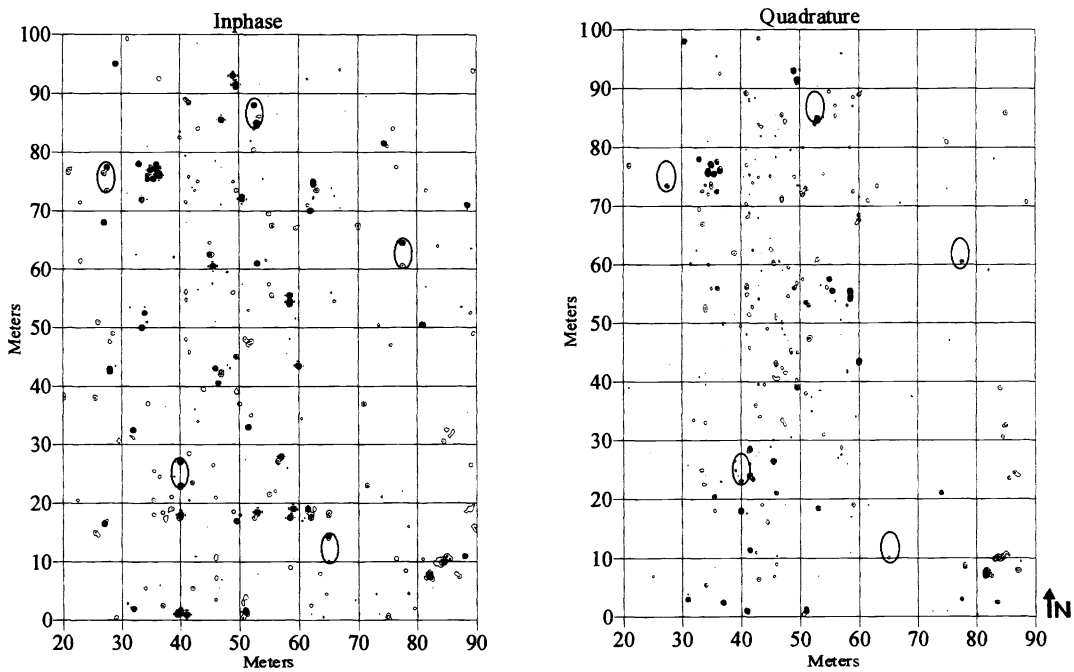

Figure 6. GEM-3M data; 12,270 Hz. The open ovals indicate the locations of the registration targets

Acknowledgments

The Night Vision Directorate, U.S. Army, under SBIR Phase I Contract DAAB07-97-C-J004, is funding this research. The data from Fort A.P. Hill, VA, was obtained under a contract with the U.S. Army Waterways Experiment Station (WES), Vicksburg, Mississippi, which was, in turn, funded by the Defense Advanced Research Project Office (DARPA).

References

1. D. Patel, "Desert Storm soil propertied and mine detectors", Technical Report USA-BRDEC-TR #2537, Fort Belvoir, Unclassified, 80 pages plus appendices, 1993.
2. I.J. Won, "A sweep-frequency electromagnetic exploration method", *Development of Geophysical Exploration Methods-4*, A. A. Fitch, pp. 39-64, Elsevier Applied Science Publishers, Ltd., London, 1983.
3 I.J. Won, A wideband electromagnetic exploration method - Some theoretical and experimental results, Geophysics, v. 45, pp. 928-940, 1980.
4. I.J. Won, Keiswetter, D.A., Fields, G.R.A., and Sutton, L.C., GEM-2: A new multifrequency electromagnetic sensor, J. Environmental and Engineering Geophysics, v. 1, no. 2, pp. 129 - 138, 1996.
5. A. Witten, Won, I.J., and Norton, S., Subsurface imaging with broadband electromagnetic induction, submitted to Inverse Problems, 1997.
6. A. Witten, Won, I.J., and Norton, S., Imaging underground structures using broadband electromagnetic induction, J. Environmental and Engineering Geophysics, in press, 1997.
7. I.J. Won, D. Keiswetter, D. Hanson, E. Novikova, and T. Hall, "GEM-3: A monostatic broadband electromagnetic induction sensor", J. Environmental and Engineering Geophysics, in press, 1997.
8. I.J. Won, Apparatus and method for detecting a weak induced magnetic field by means of two concentric transmitter loops, U.S. Patent 5,557,206, 1996.
9. J. Jeans, "The mathematical theory of electricity and magnetism", pp. 431, Cambridge University Press, London, 1960.